Experimental investigation of the performance of an annular aperture and a circular aperture on the same very-small-aperture laser facet

Hongfeng Gai,[1,*] Jia Wang,[1] Qian Tian,[1] Wei Xia,[2] and Xiangang Xu[2]

[1]State Key Laboratory of Precision Measurement Technology and Instruments, Department of Precision Instruments, Tsinghua University, Beijing 100084, China
[2]Shandong University, Jinan 250100, China

*Corresponding author: gaihf99@mails.tsinghua.edu.cn

Received 11 June 2007; revised 23 July 2007; accepted 25 July 2007; posted 27 July 2007 (Doc. ID 83972); published 30 August 2007

A very-small-aperture laser (VSAL) with a circular aperture has a trade-off between the spot size and the output power. A nanometric annular aperture is fabricated to overcome this difficulty. The advantages of the annular aperture are demonstrated by measuring and comparing its near-field intensity distribution with that of a circular aperture. These apertures are fabricated on the same VSAL to ensure that they are under the same illumination conditions. The experimental results indicate that an annular aperture produces a smaller spot size and a higher peak intensity than a circular aperture. The confinement effect and the enhancement effect are attributed to the convergence of the power flow that passes through the annular aperture. The observed enhancement effect decreases when the distance from the VSAL facet is increased, but it does not vanish even when the distance is as large as 3.5 μm.

OCIS codes: 050.1220, 140.2020, 230.5590, 180.5810, 350.3950.

1. Introduction

Near-field optical storage technologies have the potential to increase current optical recording densities substantially by breaking the optical diffraction limit. A very-small-aperture laser (VSAL) has been proposed [1] for this purpose. It can produce an optical spot much smaller than the incident wavelength so it can be used for ultrahigh density optical data storage [1], heat-assisted magnetic recording [2], and superresolution near-field imaging [3]. Until now, the characteristics of a VSAL has been studied [4,5], and its performance has been analyzed [5,6].

Usually, the spot size is determined by the size of the aperture fabricated on a VSAL facet. However, the output power from a VSAL decreases dramatically when the aperture is shrunk [1,7,8]. Much effort has been made to overcome this difficulty. The first method resorts to novel shaped apertures, such as a C-aperture [9], but a C-aperture produces an asymmetric optical spot that is due to its original asymmetric structure [10–12]. The second method is to surround an aperture with periodic surface corrugations to excite surface plasmons [13–15]. Its shortcoming is that an extended surface wave pattern instead of a single optical spot is obtained [15,16]. The third method is to introduce a minute scatterer in the center of an aperture [17–19]. The scatterer functions as an alternative near-field source and enhances the near-field intensity by exciting localized surface plasmons [18]. The enhancement effect of the scatterer has also been attributed to the guided modes of a coaxial waveguide [20], because Fabry–Perot-like resonances have been observed in both theory [21–23] and experiments [24]. The third method is what we discuss in this paper.

Tanaka *et al.* introduced a scatterer in the center of a square aperture [18]. They found that the output power is almost doubled, and the near-field spot size is reduced simultaneously. The Tanaka *et al.* experiments [18] were carried out on a glass substrate.

0003-6935/07/256449-05$15.00/0

Hashizume and Koyama also fabricated an annular aperture on a vertical-cavity surface-emitting laser (VCSEL) [19]. Their far-field results showed that the VCSEL with an annular aperture has 1.8 times the output power of another VCSEL with a circular aperture, but they did not compare the near-field performance of these two apertures. This comparison is needed if a VSAL is to be used as a near-field device.

We present our experimental results on the near-field performance of an annular aperture and a circular aperture. These apertures were fabricated on the same VSAL facet to ensure that they are under the same illumination conditions. The experimental results demonstrate that the annular aperture can improve the near-field performance of a VSAL for both spot size and output power.

2. Fabrication of the Very-Small-Aperture Laser

We fabricated a VSAL from a multiple-quantum-well laser diode (LD) by the method proposed by Chen *et al.* [25]. The emitting wavelength of the LD is approximately 650 nm. The fabrication process involves the following steps. First, a SiO_2 layer of one-quarter optical thickness is deposited on the LD facet. The SiO_2 layer also functions as an insulating layer. Second, a 150 nm aluminum layer is sputtered on the SiO_2 layer. Therefore the light emission from the LD is totally blocked. Finally, the focused ion-beam (FIB) method is used to fabricate an annular aperture and a circular aperture in the aluminum film. The scanning electron microscope images of the VSAL are shown in Figs. 1(a) and 1(b). These images were taken from the top [Fig. 1(a)] and from the side [Fig. 1(b)]. These apertures were fabricated on the same VSAL facet. Moreover, they are equally separated from the centerline of the ridge structure as shown in Fig. 1(a). So these apertures have the same illumination conditions. The separation between these two apertures is approximately 1.2 μm. The outer diameter of the annular aperture is $D = 300$ nm, and the inner diameter is $d = 100$ nm. The designed inner column (scatterer) resembles a cone because of the tapering effect inherent in FIB milling. The circular aperture has the same outer diameter as the annular aperture.

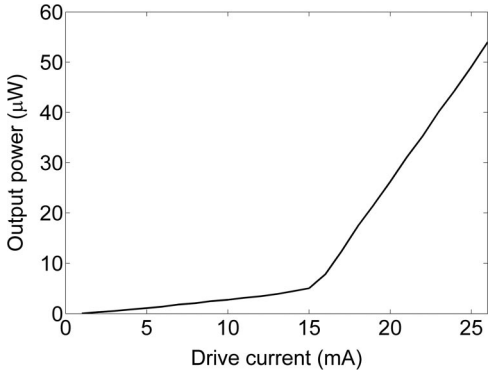

Fig. 2. Output power-drive current (P-I) curve of the VSAL. The threshold current is approximately 15.3 mA; the slope efficiency is approximately 4.6 μW/mA.

Figure 2 shows the output power-drive current (P-I) curve of the VSAL. It is obvious that the VSAL can be lased properly. The threshold current is approximately 15.3 mA, and the slope efficiency is approximately 4.6 μW/mA.

3. Experimental Results and Discussion

We measured the intensity distribution from the VSAL using a near-field scanning optical microscope (NSOM). A fiber probe was controlled to raster scan over the VSAL facet. The shear-force technology was adopted to regulate the separation between the fiber probe and the VSAL facet. The fiber probe has a tiny aperture at its apex. The diameter of the aperture is approximately 100 nm. The tapered region of the fiber probe is coated with a 100 nm aluminum film, so the apex of the fiber probe is approximately 300 nm in diameter. This value is no less than the size of the apertures. As a result, the fiber probe is outside the apertures during the scanning process, and the intensity distribution can be considered to be obtained at the constant height mode [26].

A. Confinement Effect of the Annular Aperture

The obtained near-field intensity distribution in Fig. 3(a) shows two optical spots. The left spot is from the annular aperture, and the right one is from the cir-

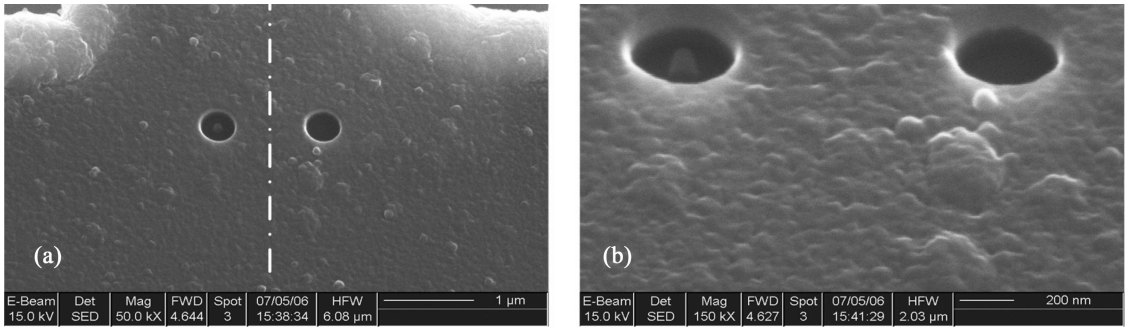

Fig. 1. (a) Top view and (b) side view of the VSAL facet with an annular aperture (left) and a circular aperture (right). The outer diameter of the annular aperture is $D = 300$ nm; the inner diameter is $d = 100$ nm. The circular aperture has the same outer diameter as the annular aperture. The separation between these two apertures is approximately 1.2 μm.

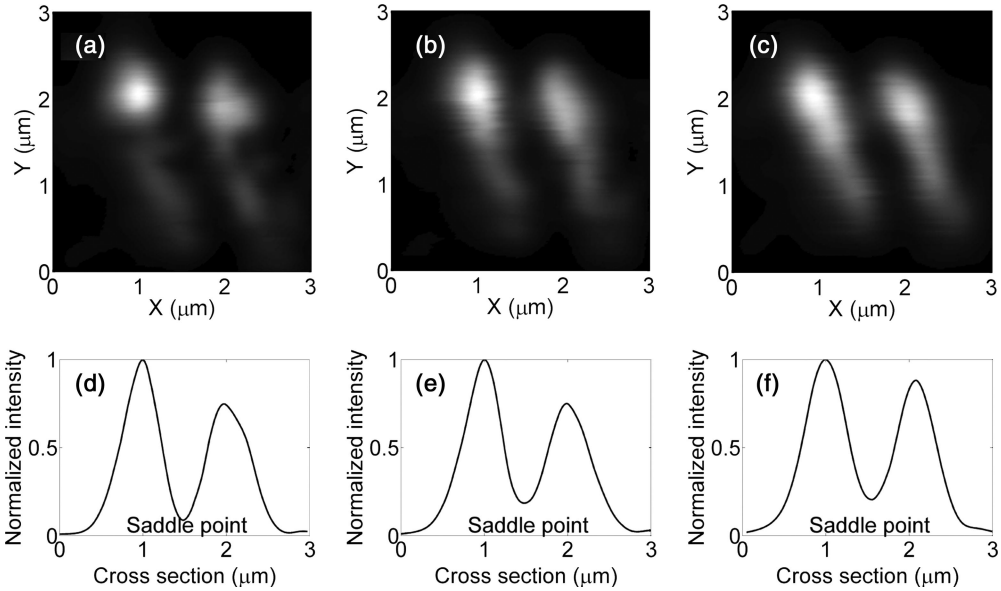

Fig. 3. Normalized intensity distribution detected at approximately (a) 0 μm (near field), (b) 1.75 μm, and (c) 3.5 μm from the VSAL facet. (d)–(f) The associated intensity profiles through the spot centers.

cular aperture. The spot sizes [(FWHM) full width at half-maximum] are 531 nm × 576 nm and 613 nm × 744 nm for the annular aperture and the circular aperture, respectively. In general, the intensity distribution is enlarged by the finite size of the fiber probe [12] so the spatial resolution of the fiber probe (approximately 100 nm) is usually subtracted from the spot sizes to obtain the net spot sizes [19]. In this way one can estimate the net spot sizes to be 431 nm × 476 nm and 513 nm × 644 nm, respectively. The experimental results indicate that the annular aperture confines the optical near field better than the circular aperture. This conclusion is in satisfactory agreement with the Tanaka *et al.* experimental results [18]. Tanaka *et al.* obtained an optical spot whose size is comparable with the size of the scatterer [18], whereas our optical spots are much larger. This could be because the Tanaka *et al.* aperture was fabricated on a glass substrate [18], whereas our apertures are fabricated on the VSAL, which is a more practical approach.

B. Enhancement Effect of the Annular Aperture

The annular aperture not only confines the optical near field effectively but also satisfactorily enhances the output power. Figure 3(a) shows that the peak intensity of the annular aperture is larger than the peak intensity of the circular aperture. A cross-sectional analysis is performed through the spot centers to demonstrate this enhancement effect more clearly. The associated result is shown in Fig. 3(d). The enhancement factor is calculated to be 1.34. This value is in reasonable agreement with the Tanaka *et al.* experimental results [18]. It should be noted that the fiber aperture has a finite size; it collects the optical power within an area below the fiber aperture, so the enhancement factor denotes only an average enhancement effect.

The physical area of the annular aperture is $\pi(D^2 - d^2)/4$, and the physical area of the circular aperture is $\pi D^2/4$. Although the annular aperture is smaller than the circular aperture, the annular aperture delivers more power than the circular aperture. The extra power delivered by the scatterer can be estimated in the following way. The output power from the VSAL is 54 μW when the drive current is 26 mA. The power transmitted through the annular aperture is estimated to be $[54 \times 1.34/(1.34 + 1)] \approx 31$ μW. The remaining 23 μW passes through the circular aperture so the power difference of $31 - 23 = 8$ μW is introduced by the scatterer. This power difference is approximately 34.8% of the power transmitted through the circular aperture. Therefore it is obvious that the introduction of the scatterer can enhance the output power.

The annular aperture and the circular aperture are equally separated from the centerline of the ridge structure as shown in Fig. 1(a). Their illumination conditions should be the same. Since the annular aperture has a smaller physical area than the circular aperture, it should have a lower incident power. But our experimental results demonstrate that the annular aperture can deliver more power than the circular aperture. So the transmission efficiency of the annular aperture is larger than the transmission efficiency of the circular aperture.

C. Localization of the Enhancement Effect of the Annular Aperture

In general, a near-field enhancement effect is accompanied by its localization. That is, the enhancement effect decreases when the distance from the VSAL facet increases. We measured the intensity distribution at different heights to analyze the localization of the enhancement effect of the annular aperture. The

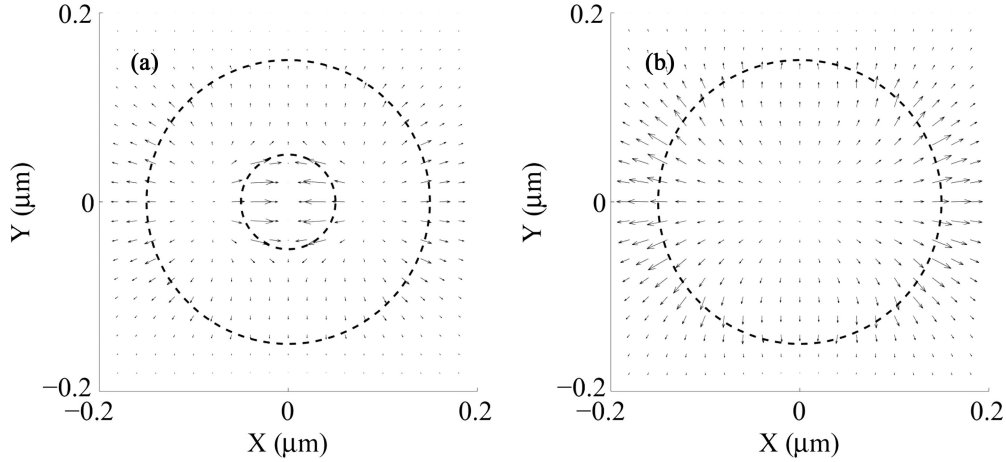

Fig. 4. Poynting vector plot of (a) the annular aperture and (b) the circular aperture in a plane 5 nm behind the apertures. The dashed lines denote the location of the apertures.

enhancement factors are calculated and compared at these locations. Our NSOM system has a limitation: the separation between the fiber probe and the VSAL facet cannot be regulated when the fiber probe enters the near-field region. Alternatively we control the fiber probe to gradually approach the VSAL facet. The approaching process is implemented by use of a stepper motor whose minimum step is 1.75 μm. The intensity distributions of approximately 0 (near field), 1.75, and 3.5 μm from the VSAL facet are depicted in Figs. 3(a)–3(c), respectively. The associated intensity profiles are shown in Figs. 3(d)–3(f), respectively. The enhancement factor decreases from 1.34 to 1.33 and 1.13 when the distance increases, indicating that the localization of the enhancement effect does exist. Fortunately, the annular aperture continues to deliver more power than the circular aperture, even at a distance of 3.5 μm from the VSAL facet.

One might wonder whether there is some interference for the field pattern because the two apertures have such a small separation. Moreover, if the interference does exist, will it influence the experimental results? We believe that the interference is negligible, if it does exist. The evidence is as follows. First, no interference fringes can be observed from the experimental results shown in Figs. 3(a)–3(c). Second, since the separation between the two apertures is approximately twice that of the emitting wavelength, there should be another three peaks in Figs. 3(d)–3(f) if the interference is strong enough. That is, altogether there should be five peaks instead of two. However, we observe only one saddle point instead of the extra three peaks. In addition, the saddle point is much lower than the surrounding two peaks.

D. Finite-Difference Time-Domain Simulations

Finite-difference time-domain (FDTD) simulations are performed to explain the confinement effect and the enhancement effect of the annular aperture. Commercial software XFDTD V6.2 was used for the simulations. The dispersive behavior of aluminum is described by the modified Debye model [27]. The infinite frequency relative permittivity, zero frequency relative permittivity, conductivity, and relaxation time are 1.8614, −656.21, 5.4455×10^6 S/m, and 1.07×10^{-15} s, respectively [28]. The simulation volume was divided into 5 nm × 5 nm × 5 nm cubic cells. The Liao absorbing boundary condition [29] was applied to all sides of the simulation volume. The excitation source is an optical plane wave polarized along the x direction. The time step is 8.66625×10^{-18} s.

Figures 4(a) and 4(b) show the Poynting vector distributions from the annular aperture and the circular aperture, respectively. The plane of the plot is 5 nm behind the apertures. In Figs. 4(a) and 4(b) the dashed lines denote the locations of the apertures, the directions of the arrows denote the power flow direction, and the length of the arrows denotes the magnitude of the Poynting vector. It can be seen that the light that passes through the gap region of the annular aperture converges on the scatterer. In contrast, the light that passes through the circular aperture diverges. So the annular aperture can concentrate light to a small optical spot with large peak intensity. Further research is necessary to explain why the annular aperture can converge the power flow.

4. Conclusion

In summary, an annular aperture was fabricated to improve the near-field performance of a VSAL in spot size and output power. A circular aperture was also fabricated on the same VSAL as a reference. The advantages of the annular aperture were demonstrated by comparing the intensity distribution of these two apertures. A NSOM system was used for the measurements. Our experimental results show that the net spot size was reduced from 513 nm × 644 nm to 431 nm × 476 nm when the scatterer was introduced into the circular aperture. At the same time, the peak intensity was improved by 1.34 times. The reduced spot size and the improved peak intensity make it possible to overcome the trade-off

between spot size and output power. The FDTD simulation results indicate that the confinement effect and the enhancement effect are due to the convergence of the power flow that passes through the annular aperture. The experimental results also show that the annular aperture continues to deliver more light than the circular aperture, in spite of the localization of its enhancement effect.

This research is supported by the National Natural Science Foundation of China under grant 60678028 and the Hi-Tech Research and Development Program of China under grant 2003AA311132. The authors thank Jun Xu of Peking University, China, for fabricating the VSALs by use of the FIB method.

References

1. A. Partovi, D. Peale, M. Wuttig, C. A. Murray, G. Zydzik, L. Hopkins, K. Baldwin, W. S. Hobson, J. Wynn, J. Lopata, L. Dhar, R. Chichester, and J. H.-J. Yeh, "High-power laser light source for near-field optics and its application to high-density optical data storage," Appl. Phys. Lett. **75,** 1515–1517 (1999).
2. W. A. Challener, T. W. McDaniel, C. D. Mihalcea, K. R. Mountfield, K. Pelhos, and I. K. Sendur, "Light delivery techniques for heat-assisted magnetic recording," Jpn. J. Appl. Phys. Part 1 **42,** 981–988 (2003).
3. Q. Gan, G. Song, G. Yang, Y. Xu, J. Gao, Y. Li, Q. Cao, L. Chen, H. Lu, Z. Chen, W. Zeng, and R. Yan, "Near-field scanning optical microscopy with an active probe," Appl. Phys. Lett. **88,** 121111 (2006).
4. T. Ohno, A. V. Itagi, F. Chen, J. A. Bain, and T. E. Schlesinger, "Characterization of very small aperture GaN lasers," Proc. SPIE **5380,** 393–402 (2004).
5. H. Gai, J. Wang, Q. Tian, W. Xia, X. Xu, S. Han, and Z. Hao, "Experimental research on the performance of a very-small-aperture laser," J. Microsc. to be published.
6. Q. Gan, G. Song, Y. Xu, J. Gao, Q. Cao, X. Pan, Y. Zhong, G. Yang, X. Zhu, and L. Chen, "Performance analysis of very-small-aperture lasers," Opt. Lett. **30,** 1470–1472 (2005).
7. H. A. Bethe, "Theory of diffraction by small holes," Phys. Rev. **66,** 163–182 (1944).
8. C. J. Bouwkamp, "On Bethe's theory of diffraction by small holes," Philips Res. Rep. **5,** 321–332 (1950).
9. X. Shi, R. L. Thornton, and L. Hesselink, "Nano-aperture with 1000× power throughput enhancement for very small aperture laser system (VSAL)," Proc. SPIE **4342,** 320–327 (2002).
10. A. V. Itagi, D. D. Stancil, J. A. Bain, and T. E. Schlesinger, "Ridge waveguide as a near-field optical source," Appl. Phys. Lett. **83,** 4474–4476 (2003).
11. Z. Rao, J. A. Matteo, L. Hesselink, and J. S. Harris, "A C-shaped nanoaperture vertical-cavity surface-emitting laser for high-density near-field optical data storage," Proc. SPIE **6132,** 61320 (2006).
12. F. Chen, A. Itagi, J. A. Bain, D. D. Stancil, T. E. Schlesinger, L. Stebounova, G. C. Walker, and B. B. Akhremitchev, "Imaging of optical field confinement in ridge waveguides fabricated on very-small-aperture laser," Appl. Phys. Lett. **83,** 3245–3247 (2003).
13. L. Stebounova, F. Chen, J. Bain, T. E. Schlesinger, S. Ip, and G. C. Walker, "Field localization in very small aperture lasers studied by apertureless near-field microscopy," Appl. Opt. **45,** 6192–6197 (2006).
14. J. Gao, G. Song, Q. Gan, B. Guo, and L. Chen, "Surface plasmon modulated nano-aperture vertical-cavity surface-emitting laser," Laser Phys. Lett. **4,** 234–237 (2007).
15. S. Shinada, J. Hashizume, and F. Koyama, "Surface plasmon resonance on microaperture vertical-cavity surface-emitting laser with metal grating," Appl. Phys. Lett. **83,** 836–838 (2003).
16. L.-B. Yu, D.-Z. Lin, Y.-C. Chen, Y.-C. Chang, K.-T. Huang, J.-W. Liaw, J.-T. Yeh, J.-M. Liu, C.-S. Yeh, and C.-K. Lee, "Physical origin of directional beaming emitted from a subwavelength slit," Phys. Rev. B **71,** 041405 (2005).
17. K. Tanaka, T. Ohkubo, M. Oumi, Y. Mitsuoka, K. Nakajima, H. Hosaka, and K. Itao, "Numerical simulation on read-out characteristics of the planar aperture-mounted head with a minute scatterer," Jpn. J. Appl. Phys. Part 1 **40,** 1542–1547 (2001).
18. K. Tanaka, H. Hosaka, K. Itao, M. Oumi, T. Niwa, T. Miyatani, Y. Mitsuoka, K. Nakajima, and T. Ohkubo, "Improvements in near-field optical performance using localized surface plasmon excitation by a scatterer-formed aperture," Appl. Phys. Lett. **83,** 1083–1085 (2003).
19. J. Hashizume and F. Koyama, "Plasmon enhanced optical near-field probing of metal nanoaperture surface emitting laser," Opt. Express **12,** 6391–6396 (2004).
20. H. Caglayan, I. Bulu, and E. Ozbay, "Extraordinary grating-coupled microwave transmission through a subwavelength annular aperture," Opt. Express **13,** 1666–1671 (2005).
21. F. I. Baida and D. Van Labeke, "Light transmission by subwavelength annular aperture arrays in metallic films," Opt. Commun. **209,** 17–22 (2002).
22. F. I. Baida and D. Van Labeke, "Three-dimensional structures for enhanced transmission through a metallic film: annular aperture arrays," Phys. Rev. B **67,** 155314 (2003).
23. F. I. Baida, D. Van Labeke, G. Granet, A. Moreau, and A. Belkhir, "Origin of the super-enhanced light transmission through a 2-D metallic annular aperture array: a study of photonic bands," Appl. Phys. B **79,** 1–8 (2004).
24. M. J. Lockyear, A. P. Hibbins, J. R. Sambles, and C. R. Lawrence, "Microwave transmission through a single subwavelength annular aperture in a metal plate," Phys. Rev. Lett. **94,** 193902 (2005).
25. F. Chen, J. Zhai, D. D. Stancil, and T. E. Schlesinger, "Fabrication of very small aperture laser (VSAL) from a commercial edge emitting laser," Jpn. J. Appl. Phys. Part 1 **40,** 1794–1795 (2001).
26. E. X. Jin and X. Xu, "Enhanced optical near field from a bowtie aperture," Appl. Phys. Lett. **88,** 153110 (2006).
27. K. S. Kunz and R. J. Luebbers, *The Finite Difference Time Domain Method for Electromagnetics* (CRC Press, 1993).
28. H. Gai, J. Wang, and Q. Tian, "Modified Debye model parameters of metals applicable for broadband calculations," Appl. Opt. **46,** 2229–2233 (2007).
29. Z. P. Liao, H. L. Wong, G. P. Yang, and Y. F. Yuan, "A transmitting boundary for transient wave analysis," Sci. Sin. **28,** 1063–1076 (1984).